2021 Joint International EUROSOI Workshop and International Conference on Ultimate Integration on Silicon (EuroSOI-ULIS) | 978-1-6654-3745-5/21/$31.00 ©2021 IEEE | DOI: 10.1109/EuroSOI-ULIS53016.2021.9560669

Temperature Increase in MRAM at Writing: A Finite Element Approach

Tomáš Hadámek
Christian Doppler Laboratory for Nonvolatile Magnetoresistive Memory and Logic at the Institute for Microelectronics TU Wien
Vienna, Austria
hadamek@iue.tuwien.ac.at

Mario Bendra
Christian Doppler Laboratory for Nonvolatile Magnetoresistive Memory and Logic at the Institute for Microelectronics TU Wien
Vienna, Austria
bendra@iue.tuwien.ac.at

Simone Fiorentini
Christian Doppler Laboratory for Nonvolatile Magnetoresistive Memory and Logic at the Institute for Microelectronics TU Wien
Vienna, Austria
fiorentini@iue.tuwien.ac.at

Johannes Ender
Christian Doppler Laboratory for Nonvolatile Magnetoresistive Memory and Logic at the Institute for Microelectronics TU Wien
Vienna, Austria
ender@iue.tuwien.ac.at

Roberto L. de Orio
Institute for Microelectronics TU Wien
Vienna, Austria
orio@iue.tuwien.ac.at

Wolfgang Goes
Silvaco Europe
Cambridgeshire, United Kingdom
wolfgang.goes@silvaco.com

Siegfried Selberherr
Institute for Microelectronics TU Wien
Vienna, Austria
selberherr@TUWien.ac.at

Viktor Sverdlov
Christian Doppler Laboratory for Nonvolatile Magnetoresistive Memory and Logic at the Institute for Microelectronics TU Wien
Vienna, Austria
sverdlov@iue.tuwien.ac.at

***Abstract* — The writing process in spin transfer torque magnetoresistive random access memories is facilitated by elevated temperatures. In this work we investigate the temperature in the free layer (FL) during switching. With our fully three-dimensional (3D) finite element method simulation approach, we numerically solve the heat transport equation coupled to the electron, spin, and magnetization dynamics and demonstrate that the FL temperature is highly inhomogeneous due to non-uniform magnetization of the FL during switching. While the average temperature in the FL can be obtained based on an average current density and an averaged potential drop across the tunnel barrier in a one-dimensional model, a fully 3D model is required to evaluate the large local temperature variations.**

Keywords — MRAM, magnetic tunnel junction, current-induced heating, heating asymmetry, temperature variations

I. Introduction

The ongoing miniaturization of semiconductor components has pushed the chip technology to its limits due to rapidly increasing leakage currents. Moreover, in the commonly employed von Neumann architecture, where the processing unit is separated from the memory, significant energy losses due to the data transfer back and forth, the so called von Neumann bottleneck, is present. The magnetoresistive random access memory (MRAM) is a promising emerging candidate to overcome these issues. MRAM is complementary metal-oxide semiconductor (CMOS) compatible [1-3] and has zero stand-by power consumption as it is intrinsically nonvolatile. It can also be integrated into logic [4] and offers a wide temperature operation range [5].

A magnetic tunnel junction (MTJ), the basic building block of MRAM cells, consists of 3 layers: a pinned ferromagnetic layer, an oxide barrier, and a free ferromagnetic layer. In spin-transfer torque MRAM (STT-MRAM) [6], relatively high current densities through the structure are required to switch the magnetization of the FL. This results in an increased temperature of the MRAM cell and mediates the switching of the FL magnetization [7,8]. On the other hand, the increased FL temperature caused by self-heating can result in an information loss as it compromises the thermal stability [8]. To preserve the data, the temperature must be rapidly relaxed after writing. In [9], the heating asymmetry in the MTJ was observed for reversed current direction. This asymmetry was further numerically studied in [10], showing a non-linear increase of the saturation temperature with increasing heating power.

In this work we investigate the inhomogeneity of the temperature in the FL at switching. This inhomogeneity can be expected due to the fast magnetization dynamics of the MRAM cell, which results in a significant inhomogeneity of the current density across the FL plane caused by non-uniform magnetization [11,12]. Moreover, during switching, the current densities change significantly due to the rapid change of the magnetization direction. Therefore, to model the temperature in MRAM, the heat transport equation has to be coupled to current, magnetization, and spin dynamics in a fully three-dimensional (3D) model.

II. Method

A. Temperature Modelling

To describe the dynamics of the temperature T in the structure at time t and position $\boldsymbol{r}$, the heat flow equation is used.

$$c_v \rho \frac{\partial T(\boldsymbol{r},t)}{\partial t} - \boldsymbol{\nabla} \cdot [\kappa \cdot \boldsymbol{\nabla} T(r,t)] = q(r,t) \qquad (1)$$

c_v, ρ, and κ stand for the heat capacity, mass density, and heat conductivity of the material, respectively. $q(r,t)$ is the heat source term. In MTJs, two main heat sources can be identified.

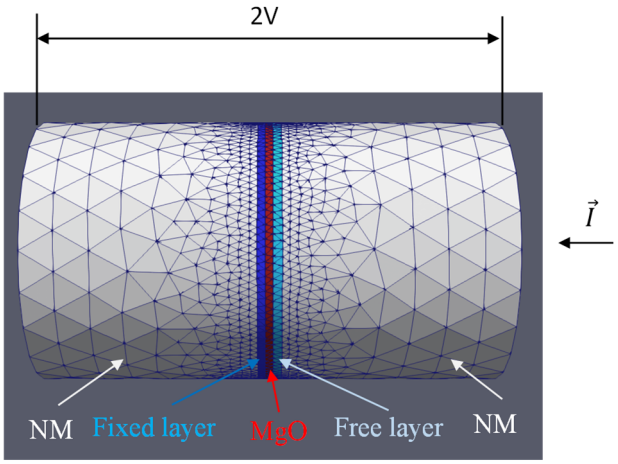

Fig. 1. The *simulated structure consisting of CoFeB(1 nm)/MgO(1 nm)/CoFeB(1.2 nm) MTJ connected to normal metal contacts (30 nm). The diameter is 40 nm. The ends are kept at a constant temperature. A bias of 2 V is applied across the structure.*

The first heat source is attributed to the Joule heat in the ferromagnetic layers and the metal contacts. It can be expressed as: $q_r(\boldsymbol{r}) = \boldsymbol{j}^2(\boldsymbol{r})\rho_{\mathrm{E}}$, where ρ_{E} is the material resistivity and $\boldsymbol{j}$ is the current density.

The second heat source is associated with electrons tunneling through the insulating barrier [7,8]. When a potential difference is applied across the MTJ, the electron tunneling from the low potential side (source) arrives at the high potential side (receiver) as a hot electron. Its energy is above the receiver Fermi energy and must be dissipated through various scattering processes. Similarly, the hole left behind the electron at the source must be filled by an electron from a higher energy level, the excess energy of which is therefore released. Setting the x-axis to coincide with the main axis along the structure, the hot electron/hole heat source is described by

TABLE I. SIMUALTION PARAMETERS - MAGNETIZATION AND SPIN

Parameter	***Value***
Gilbert damping, α	0.02
Gyromagnetic ratio, γ	$1.76\cdot10^{11}$ rad s^{-1} T^{-1}
Vacuum permeability, μ_0	$4\pi\cdot10^{-7}$ H m^{-1}
Saturation magnetization, M_S	$1.2\cdot10^{6}$ A m^{-1}
Exchange constant, A	$1\cdot10^{-11}$ J m^{-1}
Anisotropy constant, K	$0.9\cdot10^{6}$ J m^{-3}
Current spin polarization, β_σ	0.7
Diffusion spin polarization, β_D	1.0
Electron diffusion coefficient, D_e	$1\cdot10^{-4}$ m^2/s
Spin-flip length, λ_{sf}	10 nm
Spin dephasing length, λ_φ	5 nm
Exchange length, λ_J	0.5 nm
Tunnel megnetoresistance ratio (TMR)	200%

$$q_t(\boldsymbol{r}) = \left(1 \pm \alpha(\Delta U)\right)\frac{j_x(y,z)\Delta U(y,z)}{2\lambda}\exp\left(-\frac{|x - x_{F/P}|}{\lambda}\right), \quad (2)$$

where j_x and $\Delta U(y,z)$ stand for the x-component of the current density and the potential drop at the position (y,z) along FL. The x-coordinate of the position of the free/pinned-barrier interface is denoted by $x_{F/P}$ and λ is a characteristic length at which hot electrons/holes lose their energy. The heat production imbalance between the receiver and the source side is accounted for by the asymmetry coefficient $\alpha(\Delta U)$ [10]. In this work α is set to zero – no asymmetry in the receiver and source sides is considered – in order to fully investigate the details of inhomogeneous temperature development due to the non-uniform current density. The system relevant parameters are listed in Table I and Table II.

B. Magnetization Dynamic

To describe the magnetization dynamics in the micromagnetic model the Landau-Lifshitz-Gilbert equation is used.

$$\frac{\partial \boldsymbol{m}}{\partial t} = -\gamma\mu_0\,\boldsymbol{m}\times\mathbf{H}_{\mathbf{eff}} + \alpha\boldsymbol{m}\times\frac{\partial \boldsymbol{m}}{\partial t} + \frac{1}{M_S}T_{\mathrm{S}} \quad (3)$$

$\boldsymbol{m}$ is the normalized magnetization, $\gamma\mu_0$ is the scaled gyromagnetic ratio, α is the Gilbert damping, and M_S stands for the saturation magnetization. The effective filed $\mathbf{H}_{\mathbf{eff}}$ consists of several components, with the demagnetization field H_{Demag} and the anisotropy field H_{Aniso} contributing the most. In the following, H_{Demag} is determined by an optimized hybrid FEM-BEM approach [13] and H_{Aniso} is calculated with the parameters listed in Table I. T_{S} stands for the STT and couples the spin with magnetization dynamics. To determine T_{S}, the spin accumulation in the structure is computed [11,14]. The current densities and potentials were determined by solving the coupled spin, charge, and magnetization dynamics in an MTJ [12]. The described approach was implemented in a fully 3D finite element method solver based on an open source library MFEM [15]. For the time integration, an implicit Euler method was used.

III. RESULTS

In Fig. 1, the simulated structure is shown. The MTJ consisting of CoFeB(1 nm)/MgO(1 nm)/CoFeB(1.2 nm) is connected to non-magnetic metal (NM) contacts (30 nm). The outer ends of the contacts are kept at constant temperature. For the parallel to anti-parallel (P-AP) switching and anti-parallel to parallel (AP-P) switching positive and negative voltages are applied to the structure, respectively. When the voltage is applied, the electric current starts to flow through the structure and the STT acts on the free layer magnetization. Eventually, the FL magnetization is flipped.

TABLE II. SIMUALTION PARAMETERS - HEAT

	MgO	***CoFeB***	***NM***
ρ [kgm^{-3}]	3600	8200	8050
c_v [J K^{-1}kg^{-1}]	735	440	500
κ [W K^{-1}m^{-1}]	0.38	83	43
ρ_e [Ω m]	-	$2\text{x}10^{-5}$	$2\text{x}10^{-5}$
λ [nm]	-	1	1

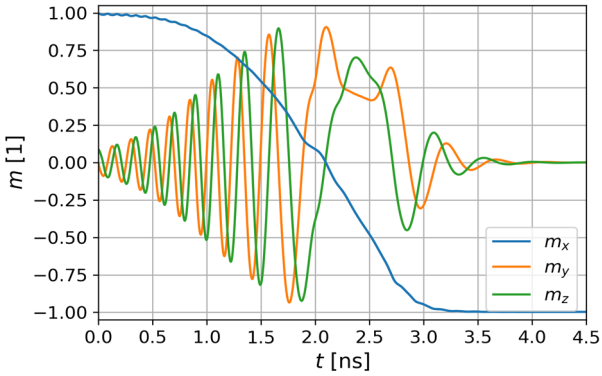

Fig. 2. Averages of normalized free-layer magnetization in x-, y- and z-direction during switching from parallel to anti-parallel. The initial magnetization was tilted by 5° in the z-direction from the x-direction to eliminate the slow incubation phase. The parallel to anti-parallel switching shows an initial oscillating behaviour.

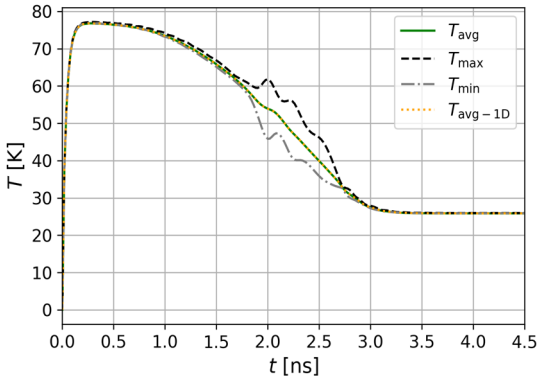

Fig. 4. Temperature in the free layer during parallel to anti-parallel switching. An average temperature T_{avg} (solid green), maximum temperature (dashed black), minimum temperature (dot-dashed grey) and T_{avg-1D} (dotted orange, coincides with green) was calculated using averages of current densities and potential drop.

Fig. 2 and Fig. 3 show the P-AP and AP-P switching, respectively. In both simulations, three different phases can be identified: Initial magnetization oscillation in the y-z plane, faster m_x component change, and a final magnetization oscillation in the y-z plane. While the fast m_x component changes are comparable in both P-AP and AP-P switching, the oscillation phases vary significantly. In the P-AP switching, the initial oscillation phase is much longer than in the AP-P switching. This is caused by an FL stabilization due to H_{Demag}, which favors the parallel orientation of the magnetic layers. Similarly, the end oscillation phase is much longer for the AP-P switching. The initial FL magnetization is tilted by 5° from the easy axis along the structure to eliminate the slow incubation phase.

Fig. 4 and Fig. 5 show the temperature development in the FL during the P-AP and AP-P switching, respectively. The average temperature T_{avg} (solid green, coincides with the dotted orange), the minimum temperature T_{min} (in dot-dashed gray) and the maximum temperatures T_{max} (in dashed black) at the FL obtained from a fully 3D model are shown. The average temperature T_{avg-1D} calculated with an average current density and an average potential drop across the barrier is also shown (dotted orange) and coincides with T_{avg} from the 3D simulations. At the beginning, a fast heating is observed after which the structure reaches thermal saturation for a specific magnetization arrangement in about 150 ps. When the saturation is achieved, the temperature in the FL changes slowly synchronously with the magnetization change. At the beginning, the temperature profile of the FL is almost homogeneous and T_{avg}, T_{min}, and T_{max} do nearly coincide. However, during the switching, an inhomogeneous temperature profile develops and T_{min} and T_{max} differ significantly. The difference is caused by the current density variations across the FL due to the non-uniform magnetization distribution shown in Fig. 6. The left plot depicts the temperature profile in the FL after 1 ns during AP-P switching. The low (high) temperature regions visible at the bottom left (top right) clearly correlate with the low (high) value regions of m_x shown in the right plot. A temperature difference of about 14 K for the applied voltage of 2 V is observed.

The ratio of the maximum temperature difference ΔT_{max} to T_{avg} in the FL is displayed in Fig. 7 and Fig. 8. In both, the P-AP and AP-P, switching simulations, this ratio increases slowly at the beginning. It then shows a sudden and considerable relative increase exceeding 30 %. After about

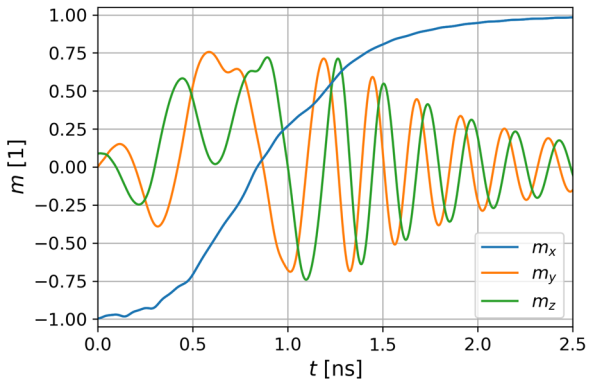

Fig. 3. Averages of normalized free-layer magnetization in x-, y- and z-direction during switching from anti-parallel to parallel. The initial magnetization was tilted by 5° in the z-direction from the x-direction to eliminate the slow incubation phase. A strong oscillating behavior is visible at the final switching phase.

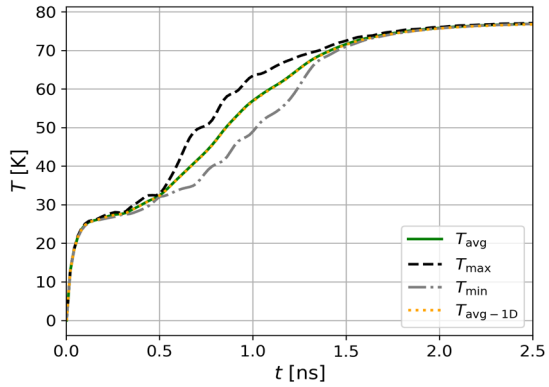

Fig. 5. Temperature in the free layer during anti-parallel to parallel swtiching. An average temperature T_{avg} (solid green), maximum temperature (dashed black), minimum temperature (dot-dashed grey) and T_{avg-1D} (dotted orange, coincides with green) was calculated using averages of current densities and potential drop.

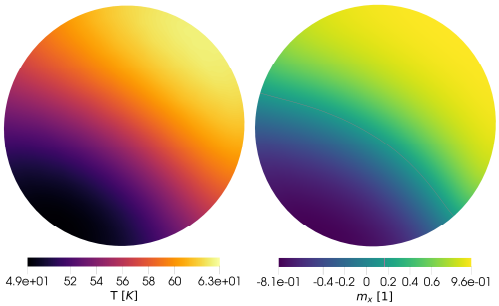

Fig. 6. Temperature profile (left) and m_x (right) in the FL at 1 ns during AP-P switching. The minimum/maximum temperature coincides with the minimum/maximum of m_x.

0.75 ns, this ratio drops again. When compared to Fig. 2 and Fig. 3, the sudden increase can easily be associated with the region of fast m_x component change, when magnetization oscillations in the y-z plane are not present.

IV. Conclusion

We have studied the FL temperature development in STT-MRAM utilizing our fully 3D finite element simulation approach coupling heat, charge, and spin transport with the magnetization dynamics. Strong temperature inhomogeneity across the FL was predicted rooting in an inhomogeneous current density distribution attributed to non-uniform magnetization of the FL. The ratio of the maximum temperature difference across the barrier to the average temperature of the FL exceeded 30 %, when the FL magnetization rapidly switches. While the average temperature in the FL can be obtained from an average current density and an average potential drop across the barrier, a fully 3D simulation is required to model the temperature variations in the FL.

Acknowledgment

Financial support by the Austrian Federal Ministry for Digital and Economic Affairs, the National Foundation for Research, Technology and Development, and the Christian Doppler Research Association is gratefully acknowledged.

References

[1] H. Ohno, "A hybrid CMOS/magnetic tunnel junction approach for non-volatile integrated circuits," 2009 Symposium on VLSI Technology, pp.122–123, August 2009

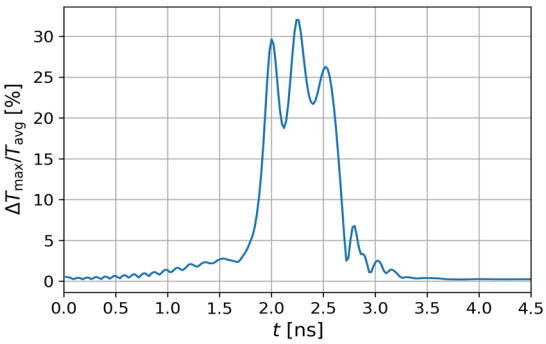

Fig. 7. Ratio of the maximum temperature difference ΔT_{max} of the free layer to the average free layer temperature T_{avg} during parallel to anti-parallel switching. ΔT_{max} reaches 30 % of the average temperature, when m_y and m_z stop to oscillate.

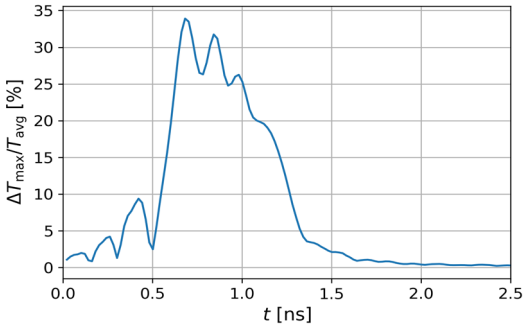

Fig. 8. Ratio of the maximum temperature difference ΔT_{SAT} of the free layer to the average free layer temperature T_{avg} during anti-paralell to parallel switching. ΔT_{max} reaches 30 % of the average temperature, when m_y and m_z stop to oscillate.

[2] K. L. Wang and P. K. Amiri, "Nonvolatile spintronics: perspectives on instant-on nonvolatile nanoelectronic systems," Spin, vol. 2, no. 2, art. no. 1250009, November 2012

[3] V. K. Joshi, P. Barla, S. Bhat and B. K. Kaushik, "From MTJ device to hybrid CMOS/MTJ circuits: A review," IEEE Access, vol. 8, pp.194105-194146, October 2020

[4] D. Suzuki, M. Natsui, A. Mochizuki, S. Miura, H. Honjo *et al.*, "Fabrication of a 3000-6-input-LUTs embedded and block-bevel power-gated non-volatile FPGA chip using p-MTJ-based logic-in-memory structure," *2015 Symposium on VLSI Circuits (VLSI Circuits)*, pp. C172–C173, June 2015.

[5] L. Thomas, G. Jan, J. Zhu, H. Liu, Y.-J. Lee, *et al.*, "Perpendicular spin transfer torque magnetic random access memories with high spin torque efficiency and thermal stability for embedded applications (invited)," Journal of Applied Physics, vol. 115, no. 17, art. no. 172615, April 2014.

[6] M. Cubukcu, O. Boulle, M. Drouard, K. Garello, C. O. Avci *et al.*, "Spin-orbit torque magnetization switching of a three-terminal perpendicular magnetic tunnel junction," Applied Physics Letters, vol. 104, no. 4, art. no. 042406, January 2014.

[7] I. L. Prejbeanu, M Kerekes, R C Sousa, H Sibuet, O Redon *et al.*, "Thermally assisted MRAM," Journal of Physics: Condensed Matter, vol. 19, no. 16, art. no. 165218, April 2007.

[8] T. Taniguchi and H. Imamura, "Thermally assisted spin transfer torque switching in synthetic free layers," Physical Review B, vol. 83, no. 5, art. no. 054432, February 2011.

[9] E. Gapihan, J. Hérault, R. C. Sousa, Y. Dahmane, B. Dieny *et al.*, "Heating asymmetry induced by tunneling current flow in magnetic tunnel junctions," Applied Physics Letters, vol. 100, no. 20, art. no. 202410, May 2012.

[10] T. Hadámek, S. Selberherr, W. Goes, V. Sverdlov, "Heating asymmetry in magnetoresistive random access memories," Proceedings of the World Multi-Conference on Systemics, Cybernetics and Informatics (WMSCI), in press, July 2021

[11] S. Fiorentini, J.Ender, S.Selberherr, R.L.de Orio, W.Goes and V.Sverdlov, "Coupled spin and charge drift-diffusion approach applied to magnetic tunnel junctions,", Solid-State Electronics, vol. 186, art. no. 108103, June 2021

[12] S. Fiorentini, J. Ender, M. Mohamedou, R. Orio, S. Selberherr *et al.*, "Computation of torques in magnetic tunnel junctions through spin and charge transport modeling", *2020* International Conference on Simulation of Semiconductor Processes and Devices (SISPAD), pp. 209-212, October 2020.

[13] D. R. Fredkin, T. R. Koehler, "Hybrid method for computing demagnetizing fields, " IEEE Transactions on Magnetics, vol. 26, no. 2, pp. 415-417, March 1990.

[14] C. Abert, M. Ruggeri, F. Bruckner, C. Vogler, G. Hrkac *et al.*, "A three-dimensional spin-diffusion model for micromagnetics, " Scientific Reports, vol. 5, art. no. 14855, October 2015.

[15] R. Anderson, J. Andrej, A. Barker, J. Bramwell, J.-S. Camiera *et al.*, "MFEM: A modular finite element library," Computers & Mathematics with Applications, vol. 81, pp.42-74, January 2021